Materials Today Communications 23 (2020) 100897

Contents lists available at ScienceDirect

Materials Today Communications

journal homepage: www.elsevier.com/locate/mtcomm

3D structure design and simulation for efficient particles capture: The influence of nanofiber diameter and distribution

Jiajun Wu[a], Obed Akampumuza[a], Penghong Liu[a], Zhenzhen Quan[a,b], Hongnan Zhang[a], Xiaohong Qin[a,*], Rongwu Wang[a], Jianyong Yu[b]

[a] Key Laboratory of Textile Science & Technology of Ministry of Education, College of Textiles, Donghua University, Shanghai, 201620, China
[b] Innovation Centre for Textile Science and Technology, Donghua University, Shanghai, 201620, China

ARTICLE INFO

Keywords:
3D structure
Simulation
Nanofiber
Electrospinning
Filtration

ABSTRACT

Software simulation is a convenient and efficient way to design and check different air filter structures with high efficiency and low pressure drop. In this work, nanofiber filters of different diameters ranging from 100 to 900 nm were designed to check their influence on filtration efficiency, pressure drop and quality factor (*QF*). Slip-flow effect of air molecules was considered on the surface of single fiber. Then, filters with different diameter distributions were constructed to study the filtration efficiency discrepancy when the filter thickness and porosity were kept equal. With a rotation of the filters composed of nanofibers of 500 nm in diameter in the computational domain, the filtration efficiency and *QF* increased steadily. The simulation results were partially verified by electrospun cellulose acetate nanofiber filter, and meanwhile provide with new insights into the filter structure design of high filtration efficiency with low pressure drop.

1. Introduction

Particulate matter 2.5 (PM 2.5) refers to tiny particles with an equivalent diameter of less than or equal to 2.5 μm in the atmosphere, which have large specific surface area, strong activity, and easy to attach toxic and harmful substances. Fig. 1 shows the distribution of the global median PM2.5 simulated concentration from World Health Organization [1]. Particles of 10 μm in diameter are usually deposited in the upper respiratory tract, and they can penetrate deep into the bronchioles and alveoli once the size are less than 2 μm, posing a great threat to human health [2]. PM 2.5 mainly come from human activities such as industrial pollution, secondary inorganic aerosol, coal combustion, biomass burning, traffic and waste incineration emission as well as the natural soil dust [3]. The composition changes with different seasons. Except for controlling air pollution from various original sources, the demand for air purified with filters is increasing with booming industrial development.

High filtration efficiency, low pressure drops and large dust holding capacity are the ideal properties for effective air filtration. Reducing the fiber diameter in filter is an efficient way to increase filtration efficiency [4]. Electrospun nanofiber filters offer a promising method for PM 2.5 capture due to their large specific surface area, small fiber diameter and tortuous pore architecture. They have fibers with diameters ranging from 50-2000 nm and mean pore sizes of around several hundred nanometers to several microns [5]. Whereas the increase of filtration efficiency with thinner fibers is desirable, the increase of pressure drop that goes hand in hand with it is unwanted. Accordingly, quality factor (*QF*) is applied to optimally balance the effect of filtration efficiency (η) and pressure drop (ΔP) [1,4].

$$QF = -\frac{ln(1-\eta)}{\Delta P} \quad (1)$$

Plenty of researches have been done focusing on filtration efficiency and *QF*. Gao et al. [6] developed a ternary structure built from scaffold nanofibers, microspheres and thin nanofibers. The filtration efficiency could go up to 99.99 % with 126.7 Pa pressure drop. The inclusion of microspheres enlarged the inter-fiber voids while the thin nanofibers increased the filter surface area for efficient particle capture. For high efficiency particulate air (HEPA) filters with a minimum removal efficiency of 99.97 % for particles greater or equal to 0.3 μm, a reduction of fiber diameter is an efficient way to increase the filtration efficiency [7]. The decrease of fiber diameter to around 60-100 nm was found to be most effective for slip-effect of air molecules on the periphery of nanofibers for low air resistance [8]. As an alternative method, the introduction of carbon nanotubes (CNTs) [9,10] or cellulose nanocrystals (CNCs) [11] in electrospun nanofiber membranes not only

* Corresponding author.
E-mail address: xhqin@dhu.edu.cn (X. Qin).

https://doi.org/10.1016/j.mtcomm.2020.100897
Received 24 November 2019; Received in revised form 2 January 2020; Accepted 3 January 2020
Available online 07 January 2020

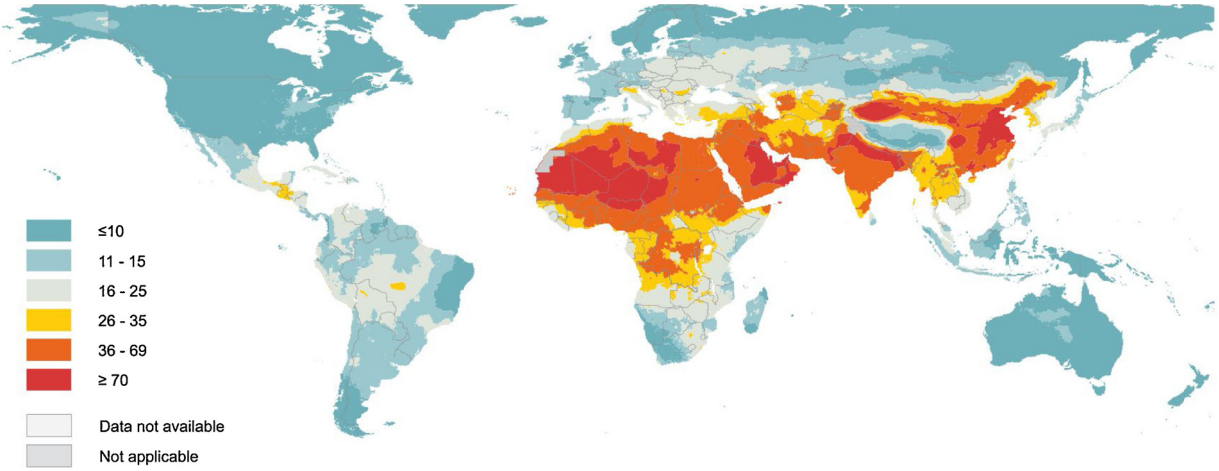

Fig. 1. World map of simulated annual PM 2.5 concentration. Reproduced with permission. [1] Copyright 2018, Elsevier.

enhanced their mechanical properties, but also greatly reduced the pressure drop. The diameter of CNTs or CNCs (from several nanometers to dozens of nanometers) is less than the mean free path of the air molecules (66 nm) which alters the Brownian diffusion of aerosol particles [12]. The incorporation of zein nanoparticles on cellulose nanofibers could also efficiently remove particles with hierarchical structure from nano to micron scale [13].

Except for structure optimization, surface modification such as electret electrospun nanofiber air filter through the implementation of corona charging, tribo-charging or low-energy-electron-beam bombardment are also regarded as promising materials for efficient particulate matter (PM) capture [14–16]. However, further improvement on the long-term effectiveness with high filtration efficiency is needed [17]. Besides, surface modification with sputtering copper or carbon on electrospun nanofiber with higher dipole moment would have better removal efficiencies to particulate matter [18]. A movable air filter system generating a high electric field would even reduce pressure drop to only several Pascal with removal efficiency over 99 % [19].

With regard to structure optimization, the hierarchical structure of nanofibers would increase the removal efficiency with tortuous pore channels to separate different sized PM [20]. A layer by layer structure with alternate different average fiber diameters was also designed to increase the filtration efficiency and *QF* [21]. High quality factor was also derived from the heterogeneous structure during the capture of various sizes of sodium hydroxide aerosols. In addition, due to a more regular pore size distribution, aligned nanofiber filter showed higher probability for particle capture than randomly oriented nanofiber membrane [22]. In this work, the influence of nanofiber diameter and its distribution on filtration properties were studied by simulation. Different 3D filter structures were designed and simulated subsequently in COMSOL Multiphysics 5.4 to check the corresponding filtration properties. The filter thickness, fiber diameter, diameter variation coefficient (*CV*) and membrane rotating angle θ were adjusted to study their relationships with filtration efficiency, pressure drop and *QF*. Finally, cellulose acetate (CA) nanofiber filters with different diameter and distribution were prepared by needleless electrospinning to verify the simulation results.

2. Methodology and simulation details

Different 3D geometric filter structures were designed in COMSOL Multiphysics 5.4. The whole process included physics selection, global parameters definition, 3D structure construction, materials attribution, boundary condition settings, meshing, study settings and results analysis. The design of the 3D geometry is shown in Fig. 2. Randomly oriented nanofibers were constructed layer by layer in a cylindrical computational region to mimic the aerosol filtration test. The filter thickness and porosity - ε (an alternative to the solid volume fraction - *SVF)* were kept the same.

$$\varepsilon = (1 - SVF)^* 100\% = \left(1 - \frac{\sum_i V_{f_i}}{V}\right)^* 100\% \quad (2)$$

Herein, *SVF* is the solid volume fraction or the percentage of the filter occupied by a single fiber of volume V_{f_i}, whereas V is the total filter volume. The tetrahedral mesh size ranges for nanofibers and computational domain were 0.0313-0.289 μm and 0.056-0.519 μm respectively. The computational domain is 10*6 μm (diameter*height) for the simulation of single fiber and single fiber diameter distribution filter analysis. The computational domain is 20*12 μm and ε was kept at 85 % for different diameter and distribution simulation. As for the simulation of filter rotation, the computational domain is 20*40 μm and ε was kept at 85 %. The upper surface of the cylinder was defined as fluid inlet while the lower surface was defined as fluid outlet. The fluid velocity was 0.053 m/s for all tests. The particles size for filtration efficiency calculation was 260 nm. It is worth mentioning that the difference between simulation and real test comes from the idealized model. Herein, the diameter of aerosol particles applied were uniform and all filtration simulations were carried out based on clean filter without clogging.

3. Material and methods

Cellulose diacetate (acetyl content 39.8 wt%) was purchased from Aladdin Reagent; acetone and N, N-Dimethylacetamide (DMAC) and dimethyl sulfoxide (DMSO) were purchased from Shanghai Lingfeng Chemical Reagent Co., Ltd.

CA (16 wt%) was fully dissolved in acetone/ N, N-Dimethylacetamide = 2/1 v/v for double needle electrospinning and acetone/ DMSO = 2/1 v/v for plate needleless electrospinning with magnetic stirring. The filter prepared by needleless electrospinning, denoted as “Filter_A”, was electrospun for 60 min at 60 kV applied voltage and 20 cm collecting distance with a collector rotating speed of 60 rpm. The filter prepared by double needle electrospinning, denoted as “Filter_B”, was electrospun at 20 kV applied voltage and 15 cm collecting distance with a collector rotating speed of 6 rpm and solution feeding speed of 0.5 mL/h. The CA solution volume was 15*2 mL for two syringes altogether. “Filter_A + B” was the combination of “Filter_A” and “Filter_B”. The samples were prepared at room temperature of 25 °C, 40 %RH and vacuum dried at 60 °C overnight before the filtration test. The nanofiber electrospinning process is illustrated in Fig. 3. Morphology of nanofibrous filters was characterized by scanning electron microscope (SEM, KYKY EM6200, China). Fiber diameter was

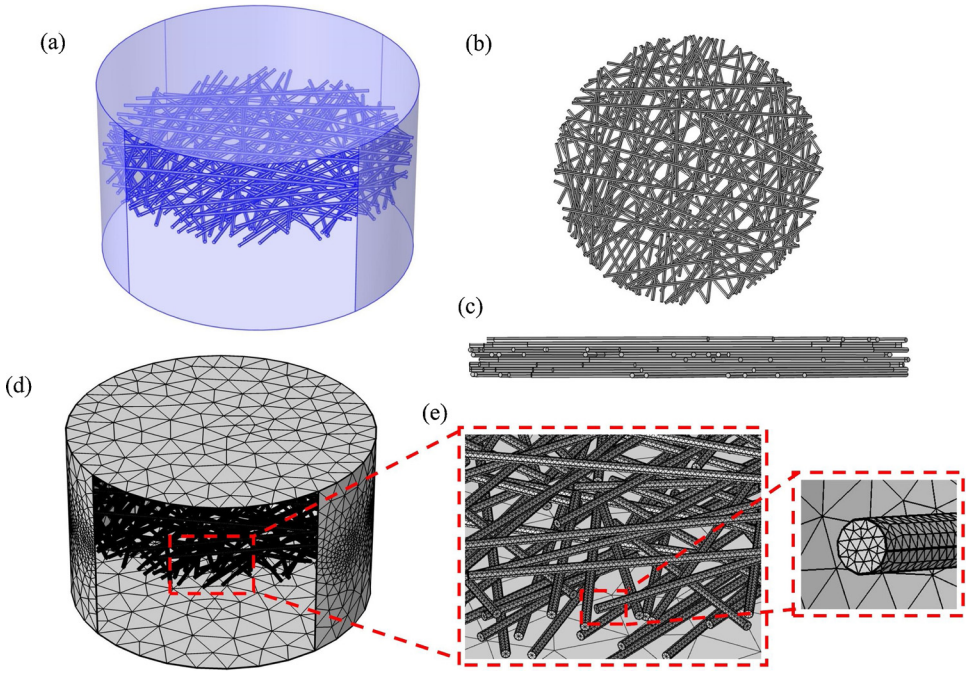

Fig. 2. (a) 3D filter of randomly oriented fibers, its (b) front view and (c) sectional view. (d) Diagram of the meshed filter and (e) its magnified portion showing the enlarged size of 100 nm nanofibers.

measured by Nano Measurer 1.2. Membrane thickness was measured by electronic micrometer. The filter pore size distribution was measured by porometer (POROLUX 100FM, Germany). Filtration efficiency and pressure drop were measured by automatic filter material tester (Certi Test 8130, USA). The median mass averaged diameter of sodium chloride aerosol was 260 nm with fluid velocity of 0.053 m/s.

4. Results and discussion

4.1. The relationship between nanofiber diameter and filtration effect

The prevailing air fluid of Stokes flow had low Reynolds number R_e here, which was given by

$$R_e = \frac{\rho v d_f}{\mu} \tag{3}$$

Herein, ρ is the fluid density (1.204 kg/m^3 at 293.15 K), v is the fluid velocity, μ is the dynamic viscosity of air (1.825*10^{-5} Pa*s) and d_f is the fiber diameter. R_e, ranging from 0.00035 to 0.00315, was far less than 1 with various fiber diameters, which could be inferred that the inertia force was far lower than viscous force [23]. The airflow field velocity distribution on the periphery of single fiber was studied for diameters ranging from 0.1 μm to 0.9 μm. As shown in Fig. 4(a)-(e), the air flow velocity magnitude on the nanofiber surface was decreasing with increasing fiber diameter, which could be ascertained from the change of blue color region area. The thinner the fiber diameter was, the less influence on the wake flow region.

In order to study the effect of fiber diameter on filtration, the filter thickness and porosity were fixed at 3.5 μm and 91 % respectively. With the decrease of fiber diameter, the filtration efficiency increased from 41.0 % to 94.2 % (see Fig. 5). This was attributed to the increase of surface area (Table 1), which increased the probability particle collision with the fiber. However, the filter pressure drops increased correspondingly from 18.5 to 413 Pa. At higher values of pressure drop, the value of *QF* greatly declined. Even when the thickness was reduced to 0.88 μm, *QF* did not improve much (Table 2). Therefore, it is not desirable to simply reduce fiber diameter as this will increase the filter's filtration efficiency at the expense high pressure drop. This has also been proven by Payen's work [24]. And the dust holding capacity would not be improved with thicker filter for the clogging issue. Various sizes of particles tend to deposit in the throat of the connective pores on the filter surface [25] (Fig. 6). Basically, thicker filters correspond with higher filtration efficiency and pressure drop with all else being equal, which has been proved by a dozen of research work

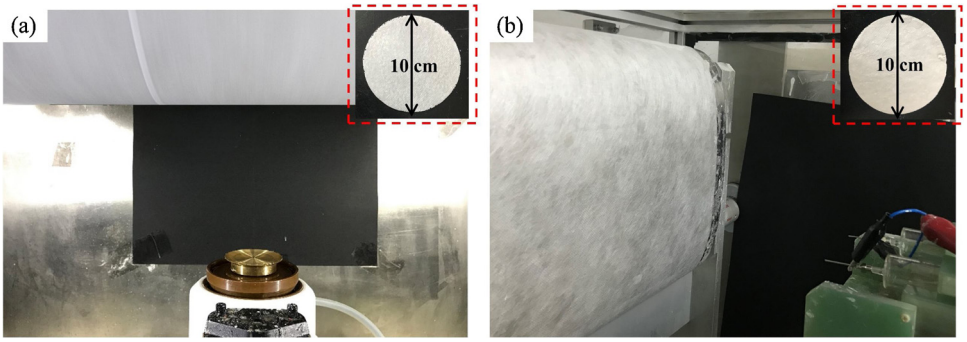

Fig. 3. CA nanofiber filter prepared by (a) needleless electrospinning with a metal plate spinneret; (b) double needle spinnerets. Upper right corner is the sample for filtration test.

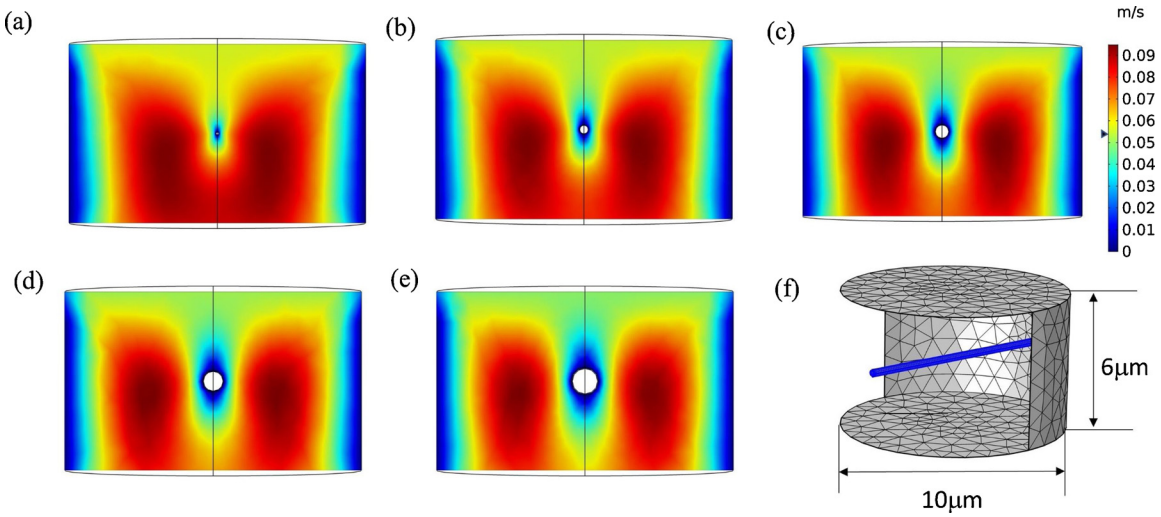

Fig. 4. Air velocity distribution around the periphery of fibers of (a) 0.1; (b) 0.3; (c) 0.5; (d) 0.7; (e) 0.9 μm in diameter. (f) The meshed calculation domain of single fiber.

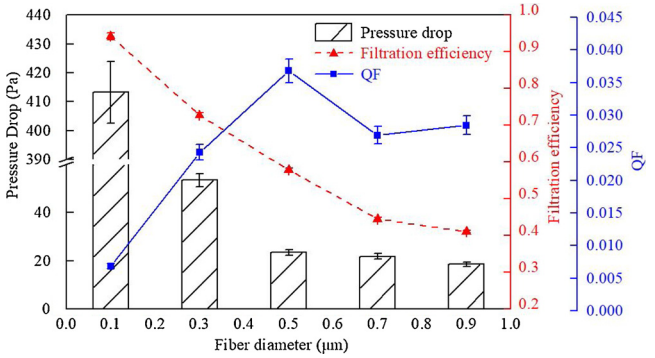

Fig. 5. The relationship of fiber diameter and pressure drop, filtration efficiency and *QF*.

Table 1
The specification of filters of various nanofiber diameter.

d_f (μm)	Surface area (μm^2)	Volume (μm^3)	Thickness (μm)	*SVF* (%)	ε (%)
0.1	1009.4.0	24.89	3.50	9.05	90.95
0.3	337.91	24.51	3.41	9.15	90.85
0.5	212.04	25.53	3.62	8.98	91.02
0.7	159.00	26.41	3.72	9.04	90.96
0.9	125.43	26.45	3.72	9.05	90.95

[4,20,22].

4.2. The relationship between nanofiber diameter distribution and filtration effect

In fact, the diameters of electrospun nanofiber are often polydisperse for the heterogeneous solvent evaporation in electrospinning bending instability process [26]. Three 3D filter structures were designed to study the fiber diameter distribution effect on filtration effect. As shown in Fig. 7, the nanofiber diameter ranged from 0.1 to 0.9 μm in "Filter_0.1-0.9", from 0.3 to 0.7 μm in "Filter_0.3-0.7" and 0.5 μm in "Filter_0.5". The quantitative weighted average diameter was 0.5 μm. With the decrease of nanofiber diameter *CV*, the fiber surface area increased steadily (see Table 3).

In Fig. 7(d)-(f), "Filter_0.5" had fewer 'big' connective pores than "Filter_0.1-0.9" and "Filter_0.3-0.7", and this is elaborated in the circled parts of Fig. 7(d) and (e). In Fig. 8, the pressure drops of different filters did not change much. However, the filtration efficiency increased steadily from 70.4 % to 73.0 % with a slight increase of *QF*. The filter of homogeneously distributed nanofiber diameters had a higher filtration efficiency due to its higher surface area and more even pore size distribution. Similar conclusion has also been reached by Wei [27] with a non-linear regression model between fiber diameter standard deviation and filtration efficiency. In his model, electrospun nanofiber filters with higher applied voltage had smaller fiber diameter standard deviation and mean pore size, which improved the filtration efficiency.

4.3. The relationship between nanofiber filter rotating angle and filtration performance

Pressure drop in air filtration is the pressure difference resulting from the air fluid velocity loss with continuous air molecule collision with the nanofiber surface. In order to reduce the magnitude of this impaction, a nanofiber filter with fibers 0.5 μm in diameter was rotated at $\theta = 30^\circ$ and then $\theta = 60^\circ$ within the computational region. The larger the rotation angle θ, the smaller was the pressure difference between front and back side of the filter. Maximum and minimum pressure on filter surface was marked with red and blue dotted boxes in Fig. 9(d)-(f). Pressure drop decreased gradually from 42.3 Pa to 24.4 Pa with increasing rotating angle in Fig. 10, while the efficiency increased from 75.3 % to 83.7 %. This was attributed to the increasing effective filtration area (Shown in Supplementary Table 1). When the filter rotated in the computational regional, the velocity component along the

Table 2
Filtration efficiency of different thicknesses of the filters.

Thickness (μm)	Pressure drop (Pa)	Filtration efficiency (%)	*QF*	Surface area (μm^2)	Volume (μm^3)	ε (%)
3.50	413.19	94.2	0.0069	1009.40	24.89	90.95
1.75	204.59	84.4	0.0091	504.68	12.44	90.95
0.88	99.743	62.5	0.0098	252.35	6.22	90.89

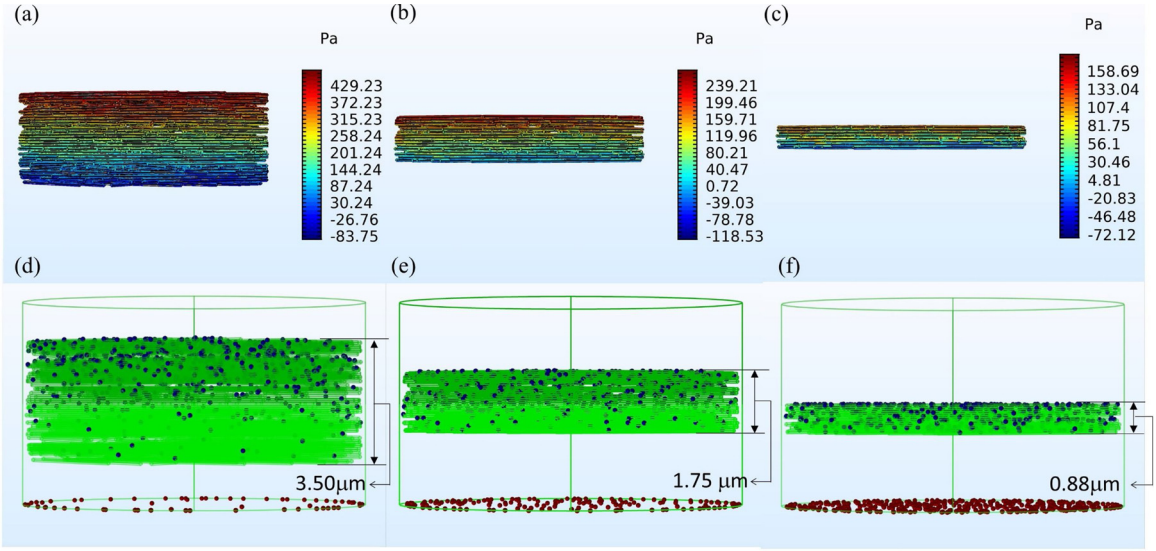

Fig. 6. Thickness influence on filter pressure drop of (a) 3.50 μm; (b) 1.75 μm; (c) 0.88 μm and their corresponding particles deposition distribution along the thickness direction.

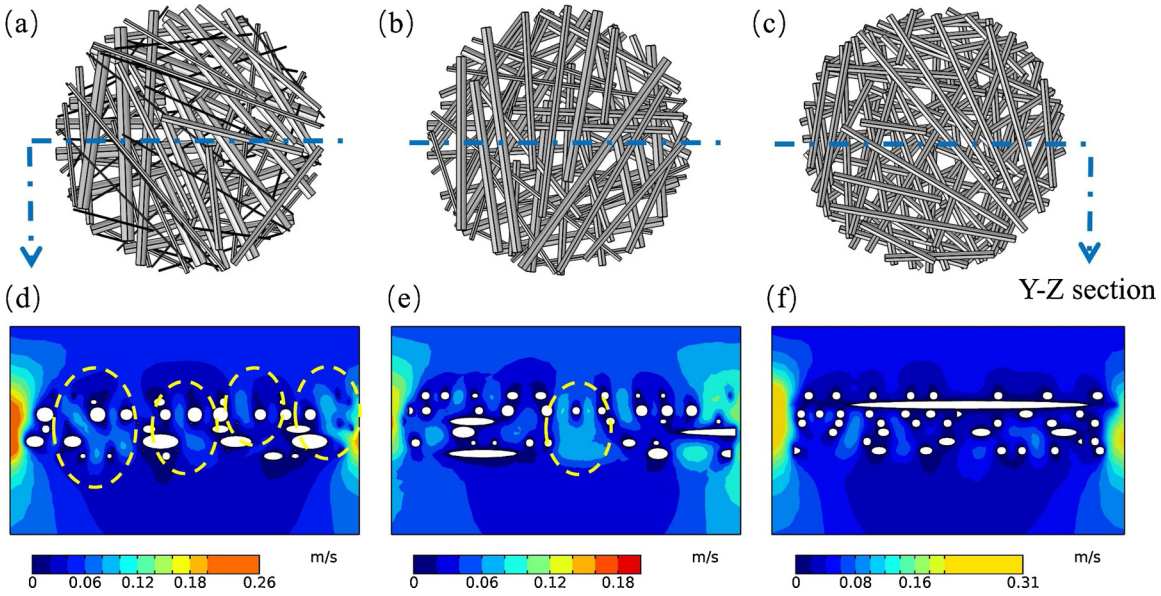

Fig. 7. The front view of different diameter distributions in filters: (a) Filter_0.1-0.9; (b) Filter_0.3-0.7; (c) Filter_0.5 and (d)-(f) their fluid velocity distribution along their Y-Z axis section.

Table 3
The specification of different diameter distribution in fibrous filters.

Diameter Range (μm)	*CV* (%)	Surface area (μm^2)	Volume (μm^3)	Thickness (μm)	ε (%)
0.1-0.9	56.7	1193.9	175.8	3.74	85.04
0.3-0.7	32.8	1311.2	174.31	3.70	85.00
0.5	0	1428.2	173.76	3.68	84.97

normal direction of the filter surface was smaller than its original velocity. Smaller velocity component along the normal direction of the filter corresponded with less impaction on filter with all else being equal. Besides, *QF* was more than doubled when the rotation angle was 60°. It can be inferred that with a zigzag shape of filter configuration, the *QF* and dust holding capacity would be greatly increased.

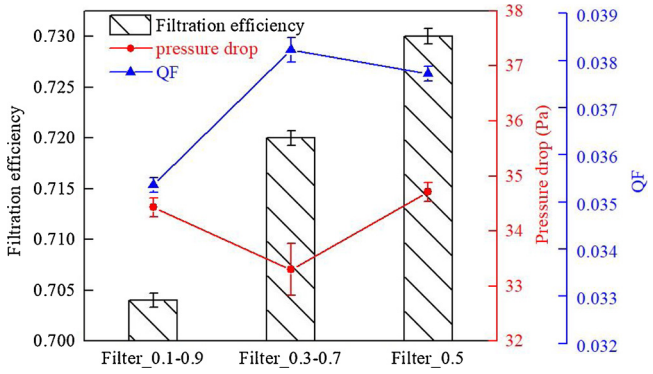

Fig. 8. The effect of using diverse diameter distributions in filters on filtration.

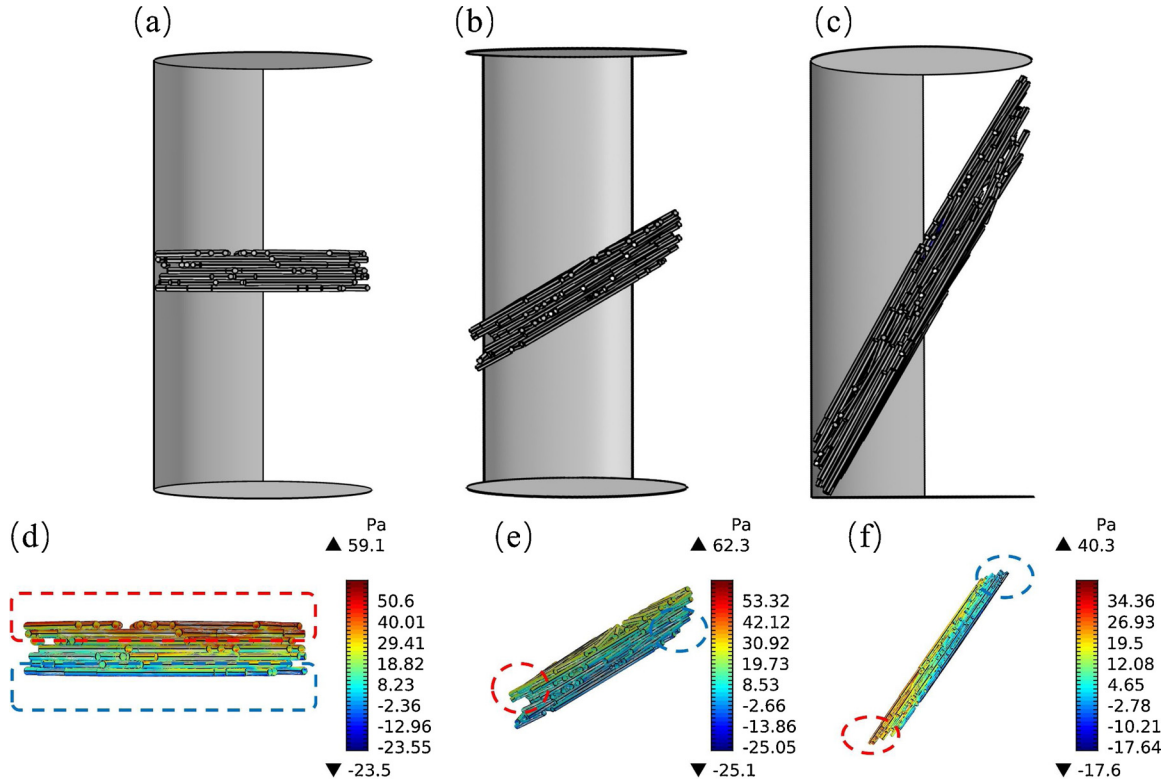

Fig. 9. The angle between filter and fluid velocity of (a) 0°; (b) 30°; (c) 60° and (d)-(f) their corresponding pressure distribution.

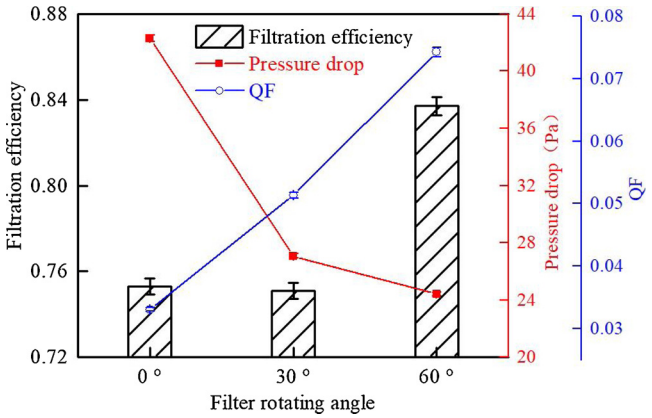

Fig. 10. The relationship between filtration properties and the rotation angle of the filters.

4.4. Filtration test of electrospun nanofiber with various diameter distribution

The cellulose acetate nanofiber was electrospun in various solution systems to obtain filters of different fiber diameter distributions. The thickness of "Filter_A" and "Filter_B" was 21.5 ± 6.5 μm and 35.8 ± 8.5 μm respectively. The thickness of "Filter_A + B" was 53.8 ± 7.7 μm. Schematic diagrams of different filter structures are given in Fig. 11(a)-(c) and their corresponding scanning electron microscope (SEM) pictures are given in Fig. 11(d)-(f). The average diameter of "Filter_A" and "Filter_B" was 203 nm and 664 nm respectively. From the diameter distribution histogram in Fig. 11(g) and (h), the nanofiber diameters in "Filter_A" ranged from 0.1-0.4 μm with *CV* of 87.2 %, while the diameter of nanofibers in "Filter_B" ranged from 0.2 to 1.5 μm with *CV* of 122.7 %.

The filter specifics are shown in Table 4. The estimated porosity of electrospun CA filter ($\hat{\varepsilon}$) was given by

$$\hat{\varepsilon}(\%) = \left(1 - \frac{w_f}{\rho_f d_m}\right) * 100\% \quad (4)$$

Herein, $\hat{\varepsilon}$ was calculated from the mean thickness d_m (m) and basis weight w_f (g/m^2) per unit area of the sample. The fiber density ρ_f is 1.3*10^6 g/m^3.

The mean pore size of "Filter_A" was about half that of "Filter_B" in Fig. 11(i). The narrower pore size and nanofiber diameter distribution accounted for the slight increase of filtration efficiency. The *QF* of "Filter_A" was much higher than that of "Filter_B", which was mainly owing to low pressure drop (shown in Fig. 12). The pressure drops increased with greater membrane thickness. Compared to "Filter_B", the filter with smaller diameter and diameter *CV* exhibited better *QF* and filtration efficiency. On the other hand, the combination of the two filters "Filter_A + B", had much higher filtration efficiency of 99.31 %. This could be explained by larger thickness and the hierarchical tortuous channels within the combined filter, which separate the aerosol of different sizes [20,21].

Combing the results in Table 4 and Fig. 12, the filtration efficiency and error of "Filter_A" were better than "Filter_B", which had proved the simulation results about the relationship between nanofiber diameter, nanofiber diameter distribution and filtration properties. The combination of the two filters in "Filter_A + B" had even higher filtration efficiency with lower *QF*, which had enlightened the researchers to balance the relationship between filtration properties and the filter structures for efficient aerosol particles capture.

5. Conclusions

In this work, we have designed and simulated the different 3D structured filters of different diameters ranging from 100 to 900 nm. The influence of nanofiber diameter and their *CV* on filtration efficiency, pressure drop and *QF* were studied based on same filter thickness and porosity. The rotation of nanofiber-based filters within the computational domain, steadily raised their filtration efficiency and *QF*.

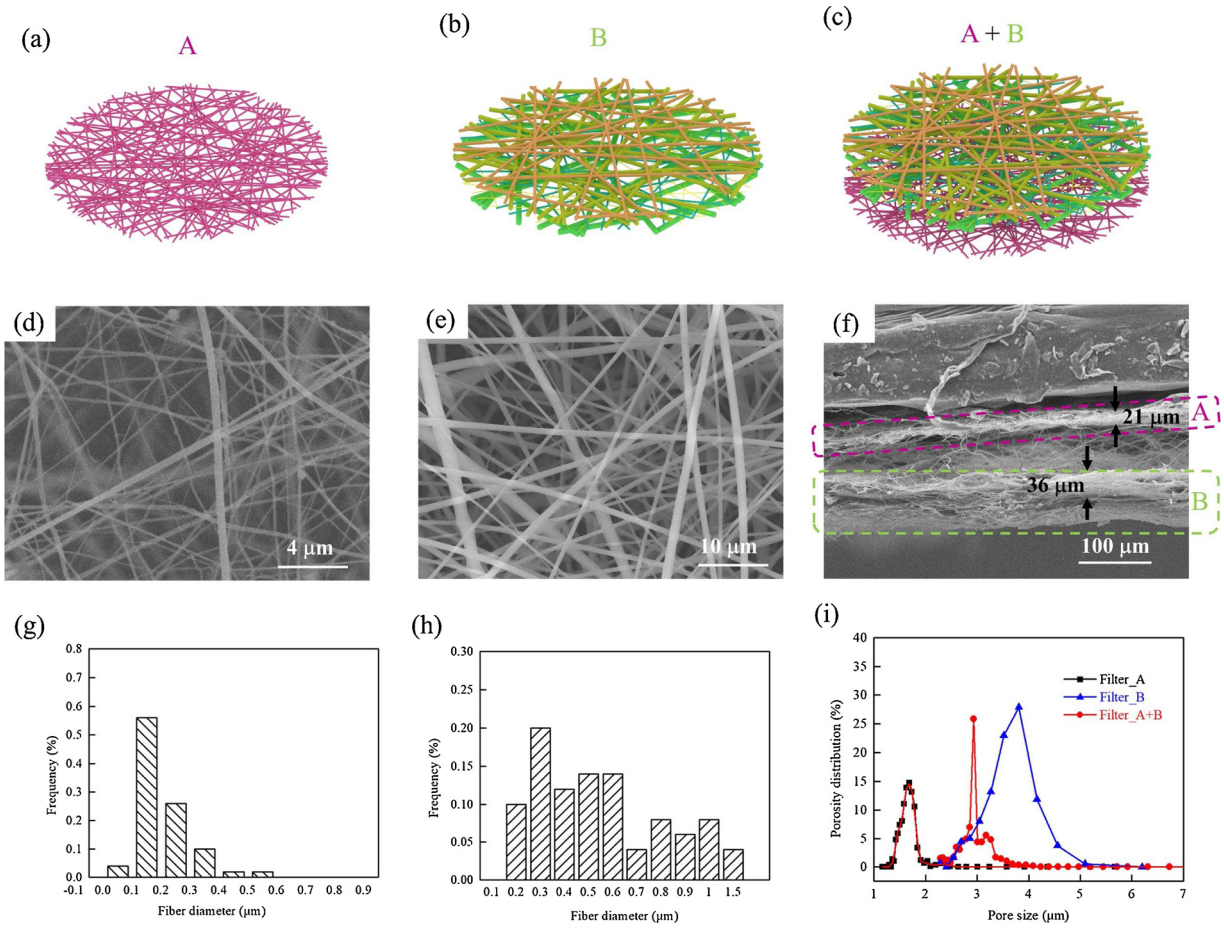

Fig. 11. The schematics of (a) Filter_A; (b) Filter_B; (c) Filter_A + B and (d)-(f) their corresponding SEM pictures. The diameter distribution of (g) Filter_A and (h) Filter_B; (i) pore distribution of different filters.

The simulation results were partially verified by electrospun cellulose acetate nanofiber filter. Meanwhile, this provides new insights into the filter structure design of high filtration efficiency and dust holding capacity with low pressure drop.

CRediT authorship contribution statement

Jiajun Wu: Writing - original draft, Formal analysis, Investigation, Data curation, Validation. **Obed Akampumuza:** Methodology, Conceptualization. **Penghong Liu:** Visualization. **Zhenzhen Quan:** Writing - review & editing. **Hongnan Zhang:** Funding acquisition. **Xiaohong Qin:** Supervision. **Rongwu Wang:** Software. **Jianyong Yu:** Project administration.

Declaration of Competing Interest

The authors declare that they have no known competing financial interests or personal relationships that could have appeared to influence the work reported in this paper.

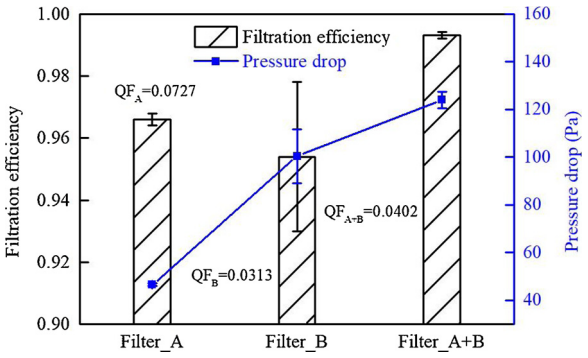

Fig. 12. The filtration effect of different filters with various diameter distributions.

Table 4
The specification of different filters.

	CV (%)	d_m (μm)	$\hat{\varepsilon}$ (%)	R^a (μm)	Δp (Pa)	η (%)	*QF* (10^{-2})
Filter_A	87.2	21.5 ± 5.6	88.48	1.75	46.55 ± 0.51	96.60 ± 0.20	7.27 ± 0.20
Filter_B	122.7	35.8 ± 8.5	87.34	3.92	100.45 ± 11.27	95.40 ± 2.60	3.15 ± 0.02
Filter_A + B	86.3	53.8 ± 7.7	87.86	2.95	123.97 ± 3.43	99.31 ± 0.11	4.02 ± 0.02

[a] *R* is the filter average pore size.

Acknowledgments

This work was supported by the Chang Jiang Youth Scholars Program of China and grants [51773037] and the general program [51973027] from the National Natural Science Foundation of China to Prof. Xiaohong Qin as well as the "Innovation Program of Shanghai Municipal Education Commission", "Fundamental Research Funds for the Central Universities" and "DHU Distinguished Young Professor Program" to her. This work has also been supported by grant [51803023, 61771123] from the National Natural Science Foundation of China to Dr. Hongnan Zhang and Prof. Rongwu Wang and the Shanghai Sailing Program [18YF 1400400], the Project funded by China Postdoctoral Science Foundation [2018M640317] and the Fundamental Research Funds for the Central Universities [2232018A3-11] to Dr. Zhenzhen Quan. It was also supported by China Scholarship Council and the PhD Innovation Foundation of Donghua University [17D310123] to Mr. Jiajun Wu.

Appendix A. Supplementary data

Supplementary material related to this article can be found, in the online version, at doi:https://doi.org/10.1016/j.mtcomm.2020.100897.

References

[1] D. Lv, M. Zhu, Z. Jiang, et al., Green electrospun nanofibers and their application in air filtration, Macromol. Mater. Eng. 303 (12) (2018).
[2] K. Yoon, B.S. Hsiao, B. Chu, Functional nanofibers for environmental applications, J. Mater. Chem. 18 (44) (2008) 5326–5334.
[3] R. Zhang, J. Jing, J. Tao, et al., Chemical characterization and source apportionment of PM2.5 in Beijing: seasonal perspective, Atmos. Chem. Phys. 13 (14) (2013) 7053–7074.
[4] W. Sambaer, M. Zatloukal, D. Kimmer, 3D air filtration modeling for nanofiber based filters in the ultrafine particle size range, Chem. Eng. Sci. 82 (2012) 299–311.
[5] S. Kaur, S. Sundarrajan, D. Rana, et al., Influence of electrospun fiber size on the separation efficiency of thin film nanofiltration composite membrane, J. Memb. Sci. 392 (2012) 101–111.
[6] H. Gao, Y. Yang, O. Akampumuza, et al., A low filtration resistance three-dimensional composite membrane fabricated via free surface electrospinning for effective PM 2.5 capture, Environ. Sci. Nano 4 (4) (2017) 864–875.
[7] R.S. Barhate, S. Ramakrishna, Nanofibrous filtering media: filtration problems and solutions from tiny materials, J. Memb. Sci. 296 (1) (2007) 1–8.
[8] X. Zhao, S. Wang, X. Yin, et al., Slip-effect functional air filter for efficient purification of PM2.5, Sci. Rep. (2016) 6.
[9] P. Li, C. Wang, Y. Zhang, et al., Air filtration in the free molecular flow regime: a review of high-efficiency particulate air filters based on carbon nanotubes, Small 10 (22) (2014) 4543–4561.
[10] O. Yildiz, P.D. Bradford, Aligned carbon nanotube sheet high efficiency particulate air filters, Carbon 64 (2013) 295–304.
[11] Q. Zhang, Q. Li, T.M. Young, et al., A novel method for fabricating an electrospun poly(Vinyl alcohol)/Cellulose nanocrystals composite nanofibrous filter with low air resistance for high-efficiency filtration of particulate matter, ACS Sustain. Chem. Eng. 7 (9) (2019) 8706–8714.
[12] P. Li, C. Wang, Y. Zhang, et al., Air filtration in the free molecular flow regime: a review of high-efficiency particulate air filters based on carbon nanotubes, Small 10 (22) (2014) 4543–4561.
[13] X. Fan, Y. Wang, W.-H. Zhong, et al., Hierarchically structured all-biomass air filters with high filtration efficiency and low air pressure drop based on pickering emulsion, ACS Appl. Mater. Interfaces 11 (15) (2019) 14266–14274.
[14] R. Thakur, D. Das, A. Das, Electret air filters, Sep. Purif. Rev. 42 (2) (2013) 87–129.
[15] S. Wang, X. Zhao, X. Yin, et al., Electret polyvinylidene fluoride nanofibers hybridized by polytetrafluoroethylene nanoparticles for high-efficiency air filtration, ACS Appl. Mater. Interfaces 8 (36) (2016) 23985–23994.
[16] G.Q. Gu, C.B. Han, C.X. Lu, et al., Triboelectric nanogenerator enhanced nanofiber air filters for efficient particulate matter removal, ACS Nano 11 (6) (2017) 6211–6217.
[17] J. Xiao, J. Liang, C. Zhang, et al., Advanced materials for capturing particulate matter: progress and perspectives, Small Methods 2 (7) (2018) 1800012.
[18] C. Liu, P.-C. Hsu, H.-W. Lee, et al., Transparent air filter for high-efficiency PM2.5 capture, Nat. Commun. 6 (1) (2015) 6205.
[19] N. Han, Y.S. Lee, B.K. Kaang, et al., A lottery draw machine-inspired movable air filter with high removal efficiency and low pressure drop at a high flow rate, J. Mater. Chem. A 7 (11) (2019) 6001–6011.
[20] M. Zhou, M. Fang, Z. Quan, et al., Large-scale preparation of micro-gradient structured sub-micro fibrous membrane with narrow diameter distribution for high-efficiency air purification, Environ. Sci. Nano 6 (12) (2019) 3560–3578.
[21] J. Xiong, M. Zhou, H. Zhang, et al., Sandwich-structured fibrous membranes with low filtration resistance for effective PM2.5 capture via one-step needleless electrospinning, Mater. Res. Express 6 (3) (2019).
[22] O. Akampumuza, H. Xu, J. Xiong, et al., Analyzing the effect of nanofiber orientation on membrane filtration properties with the progressive increase in its thickness: a numerical and experimental approach, Text. Res. J. (2019) 0040517519855316.
[23] C. Wang, Y. Otani, Removal of nanoparticles from gas streams by fibrous filters: a review, Ind. Eng. Chem. Res. 52 (1) (2013) 5–17.
[24] J. Payen, P. Vroman, M. Lewandowski, et al., Influence of fiber diameter, fiber combinations and solid volume fraction on air filtration properties in nonwovens, Text. Res. J. 82 (19) (2012) 1948–1959.
[25] D. Thomas, P. Penicot, P. Contal, et al., Clogging of fibrous filters by solid aerosol particles experimental and modelling study, Chem. Eng. Sci. 56 (11) (2001) 3549–3561.
[26] D.H. Reneker, A.L. Yarin, H. Fong, et al., Bending instability of electrically charged liquid jets of polymer solutions in electrospinning, J. Appl. Phys. 87 (9) (2000) 4531–4547.
[27] L. Wei, H. Zhang, X. Qin, Fabricated narrow diameter distribution nanofiber for an air filtration membrane using a double rings slit spinneret, Text. Res. J. 89 (6) (2019) 936–947.